ANALYZING SEPARATION LOSS EVENTS IN TWO-PAIRED AIRCRAFT TRAILING CONDUCTING AIRBORNE TIME SPACING BASED CONTINUOUS DESCENT ARRIVAL

Eri Itoh*, Kazuhiko Uejima*, Mariken Everdij, G. J. (Bert) Bakker**, and Henk Blom****
***Electronic Navigation Research Institute ENRI, Japan**
****National Aerospace Laboratory NLR, The Netherlands**

Keywords: ***Continuous descent, Interval Management, Airborne Time-spacing, Petri net, Sequential Monte Carlo simulation***

Abstract

For realizing accurate time-spacing, Aircraft Surveillance Applications System (ASAS) is seen as a promising option in the future Air Traffic Management (ATM). One ASAS application of great interest is Interval Management (IM), which provides speed commands to maintain assigned time spacing between a leading aircraft at a chosen point, for example, at a runway threshold. The questions are how safety and capacity depend on the setting of spacing criteria in the IM operation, and how to identify potential safety risks that should be taken into account in the operation design. One of the most critical situations would be in the mixture of airborne surveillance; some aircraft use ADS-B surveillance and some follow the conventional way without ADS-B data-link in the same arrival flow. Aiming to learn how to understand non-nominal properties in the IM operation, this paper furthers a mathematical modeling and large-scale simulation study. Not only the loss of ADS-B surveillance information, but also the combinations with deterioration of positioning/speed data and pilot action delays are discussed via analysis on sequence of events based on a large scale Monte Carlo simulation.

1 Introduction

Accurate time spacing between arrival aircraft increases runway capacity and operational effectiveness, and improves air traffic safety. Furthermore, it supports energy saving arrivals, often referred to as Continuous Descent Arrival (CDA), not only for one aircraft, but also for all arriving aircraft. In order to realize the assigned time spacing accurately, the Aircraft Surveillance Applications System (ASAS), which used to be called Airborne Separation Assistance System, is seen as a promising option in the future Air Traffic Management (ATM). One ASAS application of great interest is Interval Management (IM), which provides speed commands to maintain assigned time spacing between a target aircraft at a chosen point, for example, at a runway threshold [1]. Speed commands are provided by a pair-based control, with which each aircraft controls the airspeed to achieve time spacing between itself and its leading aircraft (we call it a “target” aircraft). Therefore the arrival traffic flow carrying out IM operation consists of multiple pairs of aircraft using ADS-B surveillance information. The questions are how safety and capacity depend on the setting of spacing criteria in combination with specific IM design aspects, and how to identify potential safety risks that should be taken into account in the operation design. One of the most critical situations would be in the mixture of airborne surveillance; some aircraft use ADS-B surveillance and some follow the conventional way of ATM without ADS-B data-link in the same arrival flow. More specifically, loss of a target aircraft on the ADS-B surveillance in the pair-based control could be a potential cause of

safety hazards. Analyzing risks in the non-nominal events under the loss of ADS-B connection will provide us with some speculations on estimating risks in a mixed equipped stage, for which some aircraft equips/installs hardware/software necessary in the IM operation and some do not. Aiming to learn understanding these non-nominal properties in the IM operation, this research furthers a mathematical modeling and large-scale simulation study.

In our early study, an initial mathematical model of airborne time-spacing by speed control using ADS-B surveillance information, which we call "ASAS speed control", was developed. The performance was evaluated by numerical simulation [2-6], and the simulation results showed that the ASAS speed control was one of the possible and effective applications for CDA operation. Subsequently for safety risk analysis of the IM operation, a mathematical modeling and Monte Carlo simulation study has been developed [2-6] following the Traffic Organization and Perturbation AnalyZer (TOPAZ) methodology [7]. The fragments of separation loss events and mid-air collisions have been estimated focusing on a pair of arrival aircraft [4-6]. The results obtained have shown that the probability of a mid-air collision satisfied ICAO's target level of safety under the assumptions adopted for the simulation. These early studies suggested to further TOPAZ-IM research covering the following topics: 1) Development of mathematical models is needed to mimic more realistic IM operation including uncertainties in horizontal and vertical positioning and airspeed estimates. Separation loss events were counted in a pair of aircraft [4-6], however at least two pairs of aircraft should be used to count separation loss in arrival air traffic at an airport. When an aircraft loses its target aircraft in ADS-B surveillance, switching to a nominal profile is one of the options for an evasion maneuver. 2) In addition to counting separation loss events (e.g. mid-air collision and loss of minimum separation), analyzing of sequences of events, which bring about critical hazards, will give us a deeper understanding of operation risks. These event sequence analyses help us to grasp the causes of hazard forms learning feedback to designing an even better IM operation. As stated above, this study furthers a mathematical modeling and large-scale Monte Carlo simulation study, and analyzes sequences of non-nominal events and operational safety risks in two pairs of arrival aircraft conducting CDA during the IM operation.

This paper is organized as follows. Section 2 explains the concept of airborne time spacing, ASAS, the IM application including operational procedures and scenarios adopted in this paper. Section 3 shows a mathematical modeling and event analysis study of the IM operation. Section 4 presents the Monte Carlo speeding-up algorithm and results of the large-scale Monte Carlo simulation. Concluding remarks are in Section 5.

2 Airborne-based Interval Management (IM)

2.1 Aircraft Surveillance Applications System (ASAS)

ASAS covers a range of applications which use the ADS-B datalink to allow for a gradual shift of tasks from the Air Traffic Controller (ATCo) to pilot. It consists of an integrated air-to-air, and air-to-ground system, which enables aircraft to obtain information on surrounding air traffic via ADS-B surveillance. It shifts a part of the ATCo's tasks to a pilot and allows the pilot to maintain airborne separation by visualizing traffic information in a cockpit display. Figure 1 shows this basic concept of the ASAS. Many ASAS applications are proposed to realize various types of uses in the future ATM system. For the implementation, ASAS applications

Figure 1 Basic concept of the ASAS

require new functions: airborne surveillance, data-link, communications, displays of traffic information, traffic information processing, airborne spacing and separation, and ATM functions [8]. The ATM functions include new automation systems which support pilots, for example, an automatic speed controller, trajectory generator, and strategic conflict detector.

In the IM application, the ATCo is responsible for sequencing arrival aircraft and assigning their time intervals. A pilot follows the ATCo's instructions and controls airspeed to achieve the assigned time-spacing in the air. A new type of equipment is proposed called Flight-deck Interval Management (FIM) [1], which automatically calculates the target airspeed to achieve the assigned time-spacing and to support a pilot who is responsible for the aircraft speed control.

Two different types of the ASAS speed control laws were proposed for the airborne time-spacing: in-trail following and trajectory-based laws. Figure 2 shows the in-trail following law. This controls airspeed to achieve/maintain the assigned time-interval while the aircraft tracks the target aircraft flying along the same route [9, 10]. The experimental results of several flight simulations showed that keeping constant time-spacing for the entire flight was unacceptable from an operational point of view [11]. Additionally, the in-trail following law does not consider merging points on air routes. Figure 3 explains the recent mainstream of the ASAS speed control law for the airborne time-spacing, a trajectory-based law, which controls airspeed to achieve the assigned time-interval at an assigned point, for example, at the runway threshold using ASAS equipment [12, 13].

2.2 Operational Assumptions

This paper focuses on the IM operation of three aircraft (two pairs of a leading and following aircraft) carrying out CDA in a terminal maneuvering area (TMA) or in an adjacent sector, due to the assumption that this procedure may start between the Extended-TMA entry point and the Final Approach Fix (FAF), where

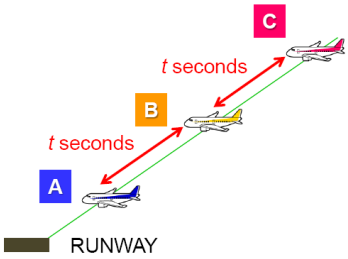

Figure 2 In-trail following law

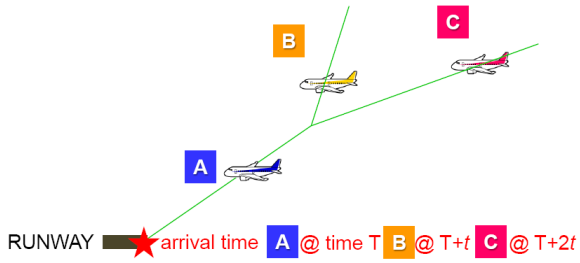

Figure 3 Trajectory-based law

the procedure should be ended. During this interval of the flight, the pilot must be aware of the surrounding traffic through ADS-B surveillance information displayed in the cockpit. The aircraft equips an ASAS director that inputs automatically its suggested speed, which is calculated in the ASAS control system, into the Autopilot System [4-6]. The pilot has then only the task of monitoring the evolution of the spacing. The ATCo gives an instruction to the pilot for identifying the target aircraft and for keeping assigned time spacing between the aircraft at a chosen waypoint.

Emergency procedures are assumed to be executed manually by the pilot. In this paper, the aircraft shifts to its planned nominal profile when it loses the target aircraft on the ADS-B surveillance.

The operational goal is to achieve an assigned time spacing τ_s at a waypoint after passing FAF (Final Approach Fix). The first aircraft follows a given nominal profile, then the others follow their target aircraft by controlling the airspeed. The first aircraft enters IAF (Initial Approach Fix) at h_e feet by v_e CAS (Calibrated Air Speed) knots, then continuously descends to the FAF by keeping a 2.5 degrees flight path. After reaching the FAF at 2,000 feet, the aircraft reduces airspeed to 180 CAS knots and increases the flap angle to 25 degrees

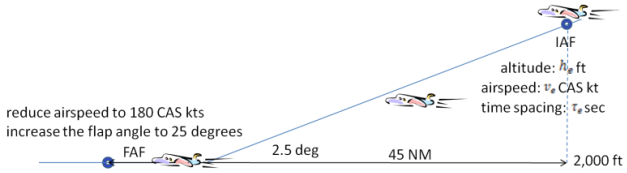

Figure 4 Operational Assumptions

proportionally in 100 seconds. The distance between IAF and FAF is 45.0 NM. The other trailing (following) aircraft enters IAF at h_e feet by v_e CAS knots τ_e seconds after the target aircraft, and trails the target aircraft while keeping τ_s seconds separation and descending to the FAF by keeping a 2.5 degrees flight path. Figure 4 shows this operation.

The dynamics and engine models are given by the AMAAI tool box [10]. The ASAS speed controller developed in Ref. [2] is used for speed control. Here we set τ_s at 90 seconds. The values, h_e, v_e, τ_e , are given by a uniform density f_U and normal density f_N as follows:

$$h_e \leftarrow f_U(x; h_{min}, h_{max}) \quad (1)$$

$$v_e \leftarrow f_N(x; v_m, \sigma_v) \quad (2)$$

$$\tau_e \leftarrow f_U(x; \tau_s - \tau_d, \tau_s + \tau_d) \quad (3)$$

Here $h_{min} = 10{,}000\ ft$, $h_{max} = 11{,}000\ ft$, $v_m = 240\ CAS\ knot$, $\sigma_v = 5\ knot$, $\tau_s =$ 90 seconds, $\tau_d = 5\ second$. f_U and f_N are as follows:

$$f_U(x; l_{min}, l_{max}) = \begin{cases} \dfrac{1}{l_{max} - l_{min}} & if\ l_{min} \le x \le l_{max} \\ 0 & else \end{cases} \quad (4)$$

2.3 Functional Characteristics

Assumptions on equipment, aircraft performance, and execution procedures are as follows: Aircraft are equipped with standard navigation and telecommunication systems, plus ADS-B, and ASAS. A simplified composition of the equipment shown in Table 1.Ground systems have the standard surveillance systems for TMA, plus the ground counterpart of ASAS. For simplicity, for the modeling and simulation in this paper all aircraft are assumed to have the performance of a B777-200.

Table 1 Aircraft Equipments

Equipment	Aircraft
SSR transponder	100%
ADS-B transmitter	100%
ADS-B receiver	100%
ASAS Spacing Director	100%
ASAS airside	100%
FMS (Flight Management System)	100%
Inertial Navigation System	100%
GNSS (Global Navigation Satellite System)	100%

3 Operation Safety Risk Modeling

3.1 Hierarchical Way of Modeling

For analyzing safety risk via a simulation study, it is necessary to make models of the IM operation, at least including generation of predicted hazards. In order to handle the complexity of the system in the mathematical modeling, we employ the hierarchical way of working to develop models. Firstly, at the top level, agents are defined, and secondly, interactions between these agents are pictured. Thirdly, each agent is modeled in further detail in several local models and their interactions. The agents and their interactions are shown in Figure 5. The six agents are described below.

Guidance, Navigation, and Control (GNC) systems agent includes three local models: *Aircraft evolution*, *FMS flight plan*, and *Aircraft guidance behavior*. The *Aircraft evolution* model shows the evolution of the aircraft that executes the IM, the *FMS flight plan* model describes the nominal flight plan of the aircraft, and the *Aircraft guidance behavior* model includes the dynamics of the aircraft including FMS, autopilot, and control systems. Initial values of aircraft speed and altitude are given by probability distributions.

Positioning systems agent includes four local models: *GPS receiver*, *Air sensor*, *Horizontal estimate*, and *Vertical estimate*. By using probability distributions, the *GPS receiver* model describes the time intervals in which the aircraft's GPS receiver is working/not working, and the *Air sensor* model describes the time

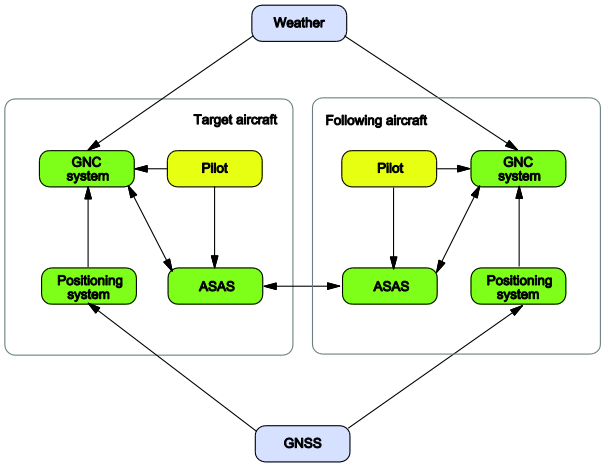

Figure 5 Agent models of the IM application

interval in which the estimation of vertical aircraft position and speed is working correctly or degraded. Based on probability distributions and dynamics given to estimate position/airspeed errors, the *Horizontal estimate* model describes the estimation error of two dimensional horizontal positions and speed of aircraft in GPS/IRS estimates, and the *Vertical estimate* model describes the estimation errors of vertical position and speed, as well as the airspeed of the aircraft. The estimation of True Air Speed (TAS) uses altitude estimated by altimeter and pitot tube measurement.

ASAS agent includes four local models: *ADS-B transmitter*, *ADS-B receiver*, *ASAS spacing*, and *ADS-B surveillance*. By using probability distributions, the *ADS-B transmitter* model describes the time interval in which the aircraft's ADS-B transmitter is working/not working, and the *ADS-B receiver* model describes the time interval in which the aircraft's ADS-B receiver is working/not working. The *ASAS spacing* model describes the dynamics of the ASAS speed controller, which automatically guides aircraft to keep certain time separation with a target aircraft, is given by ASAS space keeping criteria [2-6]. The *ADS-B surveillance* model describes the ADS-B information of all other aircraft in the ADS-B range, which aircraft update every 1second.

Pilot agent includes the *Pilot* model, which describes the action delay of a pilot until shifting to a nominal profile (following a planned flight plan) in an emergency procedure.

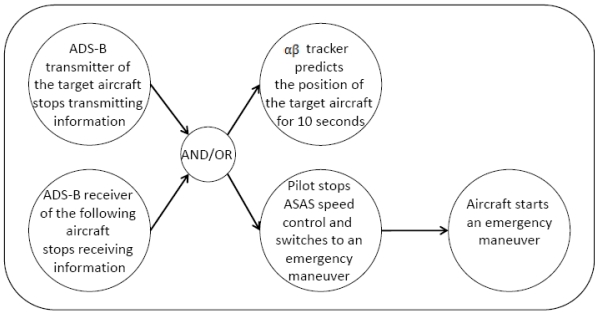

Figure 6 Hazard 1-related event sequences

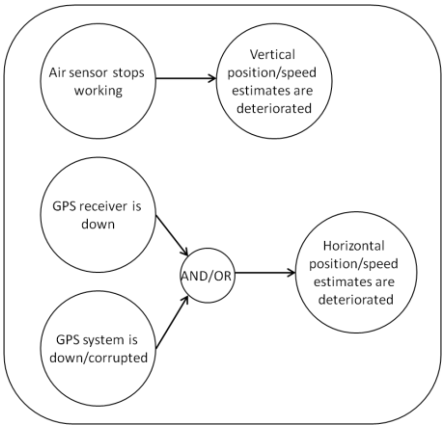

Figure 7 Hazard 2-related event sequences

GNSS agent includes the *GPS* model, which describes the time interval in which the GPS is working/degraded/corrupted/down by using a probability distribution.

Weather agent includes the*Wind* model, which describes wind dynamics in 3 directions (x, y, z on the earth axis).

These agents and their interactions are shown in Figure 5.

3.2 Local Models and Interaction Design

For the mathematical modeling of the local models and their interactions, we make use of a suitable Petri net formalism, Stochastically and Dynamically Colored Petri Net (SDCPN) [14-19], which is a Petri net extension representing a complex system including stochastic behaviors and dynamic processes. One of the powerful advantages of Petri nets is their graphical representation used in modeling a complex system in all of its components and their interactions. The SDCPN formalism allows differential equations in the models to represent the dynamic process in the applied system.

We built all the local models described in the previous section. Those models were built

to mimic at least the following two hazards in the simulation:

Hazard 1: Pilot loses a target aircraft in ADS-B surveillance during the IM operation.

Hazard 2: ASAS speed control uses deteriorated positioning and speed estimates via ADS-B surveillance.

Hazard-related event sequences are shown in Figures 6 and 7.

A combination of *ADS-B transmitter*, *ADS-B receiver*, *ADS-B surveillance*, and *pilot* model relates to the first hazard. The other combination of *GPS system*, *GPS receiver*, *Air sensor*, *Horizontal estimate*, and *Vertical estimate* model relates to the second hazard. The settings and parameters in these SDCPN models are summarized in the Appendix.

3.3 Event Analysis

Aiming to analyze causes of separation loss events, first we pick up all non-nominal events defined in the SDCPN models in Table 2 (2-1, 2-2, 2-3). As shown in the parameter settings of the SDCPN models in the Appendix, the occurrence of these non-nominal events are very rare. The additional six events defined in Table 3 are counted in the Monte Carlo simulation. Occurrences of all the events and when they happened are recorded during the simulation. Following these records, this paper discusses event combinations which cause safety critical events. Based on Tables 2 and 3, conditional probabilities of events are defined in order to discuss the sequences of non-nominal events in the next section.

Table 2-1: Definition of non-nominal events in the first aircraft

Agent	**Event**	
	ID	**Description**
ASAS agent: Communications Systems	${}^{1}E_{\mathrm{ADSt}}^{\mathrm{NW}}$	ADS-B transmitter is not working.
POSPROC agent: Positioning Systems	${}^{1}E_{\mathrm{AiP}}^{\mathrm{D}}$	Air sensor is degraded.
	${}^{1}E_{\mathrm{HoP}}^{\mathrm{D/C/I}}$	GPS estimate is degraded/corrupted or shifted to IRS estimate.

Table 2-2: Definition of non-nominal events in the second aircraft

Agent	**Event**	
	ID	**Description**
ASAS agent: Communications Systems	${}^{2}E_{\mathrm{ADSt}}^{\mathrm{NW}}$	ADS-B transmitter is not working.
	${}^{2}E_{\mathrm{ADSr}}^{\mathrm{NW}}$	ADS-B receiver is not working.
POSPROC agent: Positioning Systems	${}^{2}E_{\mathrm{AiP}}^{\mathrm{D}}$	Air sensor is degraded.
	${}^{2}E_{\mathrm{HoP}}^{\mathrm{D/C/I}}$	GPS estimate is degraded/corrupted or shifted to IRS estimate.
Pilot agent	${}^{2}E_{\mathrm{PilotAGB}}^{\mathrm{A}}$	Pilot starts evasion.
GNC agent : *Guidance systems*	${}^{2}E_{\mathrm{AGB}}^{\mathrm{E}}$	Evasion maneuver starts.

Table 2-3 Definition of non-nominal events in the third aircraft

Agent	**Event**	
	ID	**Description**
ASAS agent: Communications Systems	${}^{3}E_{\mathrm{ADSr}}^{\mathrm{NW}}$	ADS-B receiver is not working.
POSPROC agent: Positioning Systems	${}^{3}E_{\mathrm{AiP}}^{\mathrm{D}}$	Air sensor is degraded.
	${}^{3}E_{\mathrm{HoP}}^{\mathrm{D/C/I}}$	GPS estimate is degraded/corrupted or shifted to IRS estimate.
Pilot agent	${}^{3}E_{\mathrm{PilotAGB}}^{\mathrm{A}}$	Pilot starts evasion.
GNC agent : *Guidance systems*	${}^{3}E_{\mathrm{AGB}}^{\mathrm{E}}$	Evasion maneuver starts.

Table 3 Six events in the Monte Carlo simulation

Event	
ID	**Description**
${}^{2}E_{\mathrm{T0}}$	The second aircraft passes the point to start simulation (descent).
${}^{2}E_{\mathrm{T1}}$	The second aircraft passes the point to start level flight.
${}^{3}E_{\mathrm{T0}}$	The third aircraft passes the point to start simulation (descent).
${}^{3}E_{\mathrm{T1}}$	The third aircraft passes the point to start level flight.
${}^{1,2}E_{\mathrm{loss},j}$	The first aircraft and second aircraft lose defined separation at level j.
${}^{2,3}E_{\mathrm{loss},j}$	The second and third aircraft lose defined separation at level j.

4 Monte Carlo Simulation Study

4.1 Monte Carlo Speed-up Algorithm

We simulate the IM operation including the effects of non-nominal (rare) events based on the SDCPN models in the previous section. In this Monte Carlo simulation, accurate estimates of rare event probabilities should be done while avoiding lengthy computing time. ICAO's Target Level of Safety (TLS) defines a target of at most 5×10^{-9} collisions per flight hour in each of the three possible directions. In the case we count 10^{-9} order collision risk, the number of simulated samples necessary for the Monte Carlo returning valid results would be expected to be of order 10^{11}. In order to avoid lengthy computing time, appropriate techniques have to be used to speed up Monte Carlo simulations.

The technique we used for the speed-up is the Hierarchical Hybrid Interacting Particle System (HHIPS) algorithm [20] based on the importance of sampling for a large-scale stochastic hybrid system. The HHIPS incorporates sampling with modes to cope with large differences in mode weights, and the importance of switching to cope with rare mode switching. Table 4 specifies the sequence of separation loss events that have been used in the HHIPS based Monte Carlo simulations. HHIPS runs to create 5,000 samples in this paper.

Table 4 Separation loss level

Level of separation loss events	Horizontal separation distance (NM)	Vertical separation distance (ft)	Separation loss event
1	6.0	3000	No specific name
2	3.0	700	Minimum Separation Infringement (MSI) in TMA
3	1.25	500	Near Mid-Air Collision (NMAC)
4	0.3	52.5	Mid-Air Collision (MAC)

4 .2 Safety risk analysis and discussion based on simulation results

Figure 8 shows the probabilities of separation loss events obtained by the Monte Carlo simulation. The risk of mid-air collision was slightly higher than the ICAO's TLS (5.0×10^{-9}) under assumptions in this modeling and simulation study. Since any decisions made by ATCos or automation tools for pilots are not yet considered in the models, a higher risk of collision could be expected.

Figure 9 compares the Rayleigh distribution in the pilot model with a histogram of the pilot action delay obtained by the Monte Carlo simulation. The pilot model expresses the action delay before taking an emergency maneuver by a Rayleigh distribution in which the mean duration is 6.5 seconds. The mean value of the obtained time data of pilot action delay in the histogram was 15.085 seconds. As shown in Fig. 9, the centre of the histogram moves to the right side and takes bigger time values. This means that when a separation loss event happens, the pilot action of switching ASAS speed control to an emergency maneuver tends to take more time than the mean duration of the given distribution in the model. Efforts to

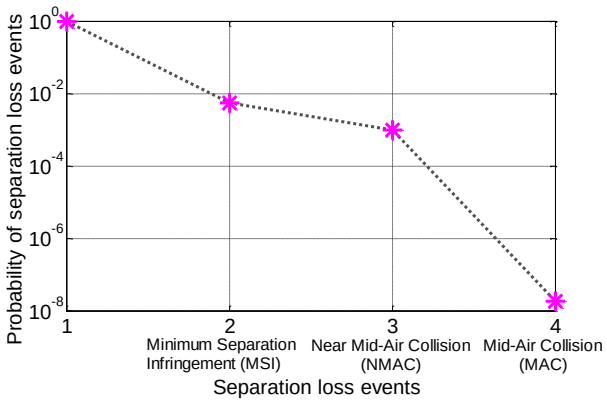

Figure 8 Probability of separation loss events per flight hour

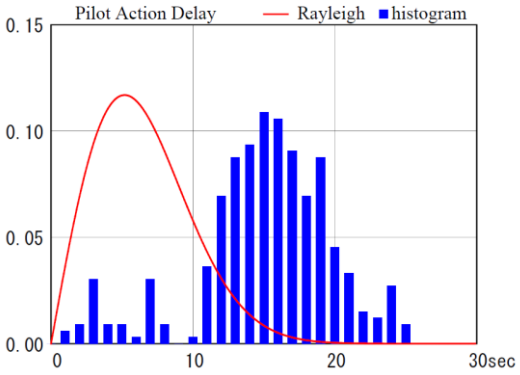

Figure 9 Rayleigh distributions in the pilot model vs. time intervals of pilot action delay when separation loss events occur.

shorten time of the pilot action delay, for example, alarm system or some other automation support, could be helpful to reduce the safety risk.

Next, conditional probabilities of events defined in Tables 2 and 3 are given to understand how and why these separation loss events occurred in the Monte Carlo simulation.

Comparison between descent flight and level flight: As shown in Figure 4, the procedure of the IM operation includes two phases, descent and level flight. The first question was which flight phase includes more risk of separation loss. By using defined events in Table 3, the probability of separation loss events which happened to the second aircraft on level flight $P_{Level,j}$ is

$$P_{Level,j} = P\left({}^{2}E_{T1} \middle| \left({}^{1,2}E_{loss,j} \cup {}^{2,3}E_{loss,j} \right) \cap \left({}^{2}E_{T0} \cap {}^{3}E_{T0} \right) \right). \quad (6)$$

Then, the probability of separation loss on descent flight $P_{Descent,j}$ is

$$P_{Descent,j} = 1 - P_{Level,j}. \quad (7)$$

Table 5 shows the value of $P_{Level,j}$ and $P_{Descent,j}$ on each level of separation loss events (Minimum Separation Infringement, Near Mid-Air Collision, and Mid-Air Collision) by percentages. As shown in Table 5, all separation loss events happened more frequently during a descent phase than during a level phase. This indicated that the non-nominal events and initial deviations have impact on a descent flight under given operational assumptions.

Table 5 Separation loss events in descent vs. level flight

	Minimum Separation Infringement	Near Mid-Air Collision	Mid-Air Collision
Descent	84.43 %	99.18 %	88.21 %
Level	15.57 %	0.82 %	11.79 %

Comparison between a former pair and latter pair: The next question was how the effect of non-nominal events propagates to the latter aircraft in a pair-based control. In this simulation the IM operation was carried out for two-pairs of aircraft (three aircraft). We compare the probability of separation loss events in the former and latter pair. Based on the events defined in Tables 2 and 3, the probability of separation loss events between the former pair $P_{Former,j}$ is

$$P_{Former,j} = P\left({}^{1,2}E_{loss,j} \middle| \left({}^{1,2}E_{loss,j} \cup {}^{2,3}E_{loss,j} \right) \cap \left({}^{2}E_{T0} \cap {}^{3}E_{T0} \right) \right) \quad (8)$$

The probability of separation loss events between the latter pair $P_{Latter,j}$ is

$$P_{Latter,j} = P\left({}^{2,3}E_{loss,j} \middle| \left({}^{1,2}E_{loss,j} \cup {}^{2,3}E_{loss,j} \right) \cap \left({}^{2}E_{T0} \cap {}^{3}E_{T0} \right) \right) \quad (9)$$

Table 6 shows the value of $P_{Former,j}$ and $P_{Latter,j}$ on each level of separation loss events by percentages. As shown in Table 6, 80.72 % of the Minimum Separation Infringement occurs between the second and third aircraft in the latter pair. After this, all Near Mid-Air Collisions and Mid-Air Collisions happened between the latter pair only. These results indicate that impacts of the non-nominal events propagated to the latter pair of aircraft. Further analysis of these stochastic behaviors will be key issues to understand the IM operation.

Table 6 Separation loss events in a former pair vs. latter pair

	Minimum Separation Infringement	Near Mid-Air Collision	Mid-Air Collision
Former pair	19.28 %	0 %	0 %
Latter pair	80.72 %	100 %	100 %

Comparison between the impacts of ADS-B surveillance failures and horizontal/vertical estimate errors: Next, we analyzed the impacts of ADS-B surveillance failures and deterioration of horizontal and vertical estimates. Using event definitions in Tables 2 and 3, the probability of ADS-B surveillance failure which causes separation loss events $P_{ADS-B\ fail,j}$ is given as

$$\begin{aligned} &P_{ADS-B\ fail,j} \\ &= P\left({}^{1}E_{ADSt}^{NW} \cup {}^{2}E_{ADSt}^{NM} \cup {}^{2}E_{ADSr}^{NW} \cup {}^{3}E_{ADSr}^{NW} \middle|^{1,2}E_{loss,j} \cap {}^{2}E_{T0} \right) \\ &+ P\left({}^{1}E_{ADSt}^{NW} \cup {}^{2}E_{ADSt}^{NM} \cup {}^{2}E_{ADSr}^{NW} \cup {}^{3}E_{ADSr}^{NW} \middle|^{2,3}E_{loss,j} \cap {}^{2}E_{T0} \cap {}^{3}E_{T0} \right). \end{aligned} \quad (10)$$

The probability of deterioration of horizontal/vertical estimates $P_{est\ error,j}$ due to a degraded air sensor, the GPS system being down, and GPS receiver being down is given as

$$\begin{aligned} &P_{est\ error,j} \\ &= P\left({}^{1}E_{AIP}^{D} \cup {}^{1}E_{Hop}^{D/C/I} \cup {}^{2}E_{AIP}^{D} \cup {}^{2}E_{Hop}^{D/C/I} \cup {}^{3}E_{AIP}^{D} \cup {}^{3}E_{Hop}^{D/C/I} \middle|^{1,2}E_{loss,j} \cap {}^{2}E_{T0} \right) \\ &+ P\left({}^{1}E_{AIP}^{D} \cup {}^{1}E_{Hop}^{D/C/I} \cup {}^{2}E_{AIP}^{D} \cup {}^{2}E_{Hop}^{D/C/I} \cup {}^{3}E_{AIP}^{D} \cup {}^{3}E_{Hop}^{D/C/I} \middle|^{2,3}E_{loss,j} \cap {}^{2}E_{T0} \cap {}^{3}E_{T0} \right). \end{aligned} \quad (11)$$

Table 7 shows the value of $P_{ADS-B\ fail,j}$, $P_{est\ error,j}$, and their combination on each level of separation loss events by percentages. As shown in Table 7, ADS-B surveillance failure was the main cause of Minimum Separation Infringement. The combination of ADS-B surveillance failure and deterioration of the horizontal and vertical estimates became 90.68 % of the cause of Near Mid-Air Collision. Then, the main cause of Mid-Air Collision was the deterioration of the estimate errors. These results indicated that the combination of non-nominal events brings the separation loss events. Data tolerance in ADS-B surveillance is one of the important factors to decide safety in the IM operation. Not only when the aircraft loses a target aircraft, but also when the level of tolerance in aircraft data is deteriorated in the ADS-B surveillance information, the decision should be made whether or not the pilot maintains ASAS speed control in the IM operation for improving the safety risk.

Table 7 Separation loss events occurred by ADS-B surveillance failure vs. positioning/speed estimates errors

	Minimum Separation Infringement	Near Mid-Air Collision	Mid-Air Collision
ADS-B surveillance failure	99.92 %	99.96 %	7.71 %
Positioning/speed estimate errors	53.89 %	90.68 %	99.96 %
Combination of ADS-B surveillance failure and positioning/speed estimate errors	53.81 %	90.64 %	7.70 %

5 Concluding Remarks

This paper developed a mathematical modeling and Monte Carlo simulation study for evaluating the IM operation for CDA. First the airborne time-spacing concept was explained including ideas on ASAS, IM application, and ASAS speed control. Under the operational assumptions, mathematical models were developed following a hierarchical way of modeling: agent models were defined and then the local models and their interactions were mathematically described following the SDCPN

formalism. Non-nominal events which possibly cause operational hazards were mathematically described in the models using stochastic distributions. The Monte Carlo simulation runs were done to create 5,000 samples implementing a speed-up algorithm based on important sampling for a large-scale stochastic hybrid system.

The results of simulation and safety risk analysis indicated that sequences of non-nominal events cause safety critical events. In this paper, deterioration of horizontal/vertical positioning and speed estimates was considered in the ADS-B surveillance data. Under the mixture of airborne surveillance; some aircraft use ADS-B surveillance and some do not, while tolerance ranges in these surveillance data relate to the probability of the separation loss events, especially in collision risk. Not only when the aircraft loses a target aircraft in the surveillance, but also when the accuracy of aircraft data was deteriorated, it could be helpful if pilots make decisions whether or not they maintain ASAS speed control depending on the tolerance level. Furthermore, supporting pilots to make decisions could be helpful in reducing the safety risk in the IM operation. One of the key issues to further investigate is how to prevent the propagation of the impacts in non-nominal events and the other stochastic behaviors in the operation of latter aircraft pairs.

In future works, updated operational assumptions will be applied to the aircraft flow arriving at airports in Tokyo via oceanic en-route, and a trajectory-based IM application will be applied. A brain-storming session will be held with operational experts, to identify additional critical hazards in the IM operation. Mathematical models will be developed to mimic at least the detected hazards. Our fast-time simulation aims to feedback vulnerability against various rare events in proposed IM operation to concept builders. Operational issues in human factors, such as the potential for confusion between controllers and pilots in high workload situations, will be investigated through real-time simulation studies complementary to this fast-time simulation study. By collaborating with concept builders and experts on real-time simulation, our approach will be further developed to evaluate the future IM application.

References

[1] RTCA, "Safety, Performance and Interoperability Requirements Document for Airborne Spacing – Flight Deck Interval Management (ASPA-FIM)", RTCA DO-328, June 22, 2011.

[2] Itoh, E., Everdij, M., Bakker, G.J., and Blom, H., "Speed Control for Airborne Separation Assistance in Continuous Descent Arrivals", *Proc. 9th American Institute of Aeronautics and Astronautics - Aviation Technology, Integration, and Operations (AIAA ATIO)*, 2009.

[3] Itoh, E., Everdij, M., Bakker, G.J., and Blom, H., "Speed Control for Airborne Separation Assistance in Continuous Descent Arrivals", R&D report published by National Aerospace Laboratory NLR Air Transport Safety Institute, NLR-TP-2010-328, September 2010.

[4] Itoh, E., Everdij, M., Bakker, G.J., and Blom, H., "The Impacts of Surveillance Failure on Airborne Separation Assistance System Based Continuous Descent Approach", *Proc. 27th International Council of the Aeronautical Science (ICAS2010)*, 2010.

[5] Itoh, E., Everdij, M., Bakker, G.J., and Blom H., "Effects of Surveillance Failure on Airborne-based Continuous Descent Approach", Journal of Aerospace Engineering, doi:10.1177/09544 1001 142 1995 (Accepted on 10 August 2011).

[6] Itoh, E., Uejima, K., Chida, H., Nishinari, K., Everdij, M., Bakker, G. J., and Blom, H., "An Overview of Airborne Time-Spacing Research in the JADE Program", *Proc*. 2nd International Conference on Application and Theory of Automation in Command and Control Systems (ATACCS 2012), May 2012.

[7] Blom, H.A.P., Bakker, G.J., Blanker, P.J.G., Daams, J., Everdij, M.H.C., and Klompstra, M.B., 'Accident risk assessment for advanced ATM', In: Air Transportation Systems Engineering, edited by G.L. Donohue and A.G. Zellweger, Vol. 193 in Progress in Astronautics and Aeronautics, Paul Zarchan, Editor-in-Chief, Chapter 29, pp. 463-480, 2001.

[8] FAA/EUROCONTROL Cooperative R&D: Action Plan 1, "Principles of Operation for the Use of Airborne Separation Assurance Systems", http://www.eurocontrol.int/care-asas/public/standard_page/art.html, 2001.

[9] CoSpace, http://www.eurocontrol.int/eec/public/standard_page/SSP_cospace_home.html

[10] Van der Geest, P., "The AMAAI Modeling Toolset for The Analysis of In-trail Following Dynamics, Deliverable D2: Description and User Guide", *NLR-CR-2002-112*, 2002.

[11] Abbott, T. "A Brief History of Airborne Self-Spacing Concepts", NASA/CR-2009-215695, 2009.
[12] Abbott, T., "A Trajectory Algorithm to Support En Route and Terminal Area Self-Spacing Concepts", NASA/CR-2007-214899, 2007.
[13] Abbott, T., "Speed Control law for Precision Terminal Area In-Trail Self Spacing", NASA/TM-2002-211742, 2002.
[14] Everdij, M.H.C. and Blom, H.A.P. "Petri Nets and Hybrid State Markov Processes in a Power-hierarchy of Dependability Models" In *Proceedings of IFAC Conference on Analysis and Design of Hybrid Systems*, Saint-Malo Brittany, France, June 2003, pp. 355–360.
[15] Everdij, M.H.C. and Blom, H.A.P., "Piecewise Deterministic Markov Processes Represented by Dynamically Coloured Petri Nets", Stochastics, Vol. 77, 2005, pp. 1–29, 2005.
[16] Everdij M.H.C. and Blom, H.A.P., "Hybrid Petri Nets with Diffusion that Have into Mappings with Generalised Stochastic Hybrid Processes", Eds: H.A.P. Blom and J. Lygeros. *Stochastic Hybrid Systems: Theory and Safety Critical Applications*, LNCIS series, Springer, Berlin, 2006, pp 31–64.
[17] Everdij, M.H.C., Klompstra, M.B., Blom, H.A.P., Klein Obbink, B., "Compositional Specification of a Multi-agent System by Stochastically and Dynamically Coloured Petri Nets", -Eds: H.A.P. Blom, J. Lygeros. *Stochastic Hybrid Systems: Theory and Safety Critical Applications*, LNCIS series, Springer, Berlin, July 2006, pp. 325–350.
[18] Everdij, M.H.C. and Blom , H.A.P., "Hybrid State Petri Nets which Have the Analysis Power of Stochastic Hybrid Systems and the Formal Verification Power of Automata", Ed: P. Pawlewski, *Petri Nets*, Chapter 12, I-Tech Education and Publishing, Vienna, 2010, pp. 227-252.
[19] Everdij, M.H.C., "Compositional Modeling using Petri Nets with the Analysis power of Stochastic Hybrid Systems", PhD thesis University of Twente, June 2010, http://www.nlr-atsi.nl/eCache/ATS/15/060.pdf.
[20] Blom, H.A.P., Bakker G.J., and Krystul, J., "Rare Event Estimation for a Large-scale Stochastic Hybrid System with Air Traffic Application, Eds: G. Rubino and B. Tuffin, Rare Event Simulation using Monte Carlo Methods", John Wiley & Sons, Ltd, chapter 9, pp. 193-214, 2009.
[21] Oliveira, I. R., Bakker, G. J., and Blom, H. A. P., "Accident Risk Assessment Model for ASAS Time-Based Spacing Operation in ATM", NLR Technical Report, NLR-TR-2006, August 2006.

Appendix

Here the parameters used in the SDCPN models which relate to two hazards defined in Section 3.2 are briefly summarized. The sources of these models are in Ref. [21].

ADS-B transmitter/receiver model describes time intervals and parameter settings in Tables A-1 and A-2.

Table A-1 Time interval in ADS-B transmitter/receiver

Time interval	Description
$f_E(\cdot;\ \mu_{ADS,TRM}^{down}(1-p_{ADS,TRM}^{down})/p_A^d$	Time interval until the ADS-B transmitter/receiver stops transmitting information.
$f_E(\cdot;\ \mu_{ADS,TRM}^{down})$	Time interval until the ADS-B transmitter/receiver starts working again.

Table A-2 Parameters in ADS-B transmitter/receiver

Parameter	Description	Value
$\mu_{ADS,TRM}^{down}$	Mean duration until the ADS-B transmitter/receiver starts working again	1/2 hour
$p_{ADS,TRM}^{down}$	Probability of ADS-B transmitter/receiver failure	1/20000

In ***ADS-B surveillance*** model, $\alpha\beta$ tracker linearly predicts a target position for 10 seconds after losing the target aircraft in the surveillance information.

Pilot model is described including time intervals and parameter settings in Table A-3 and A-4.

Table A-3 Pilot action delay

Action delay of pilot	Description
$f_R(x;\ \mu_{AC})$	Time interval until the pilot takes emergency action after ADS-B surveillance failure.

Table A-4 Parameters in pilot action delay

Parameter	Description	Value
μ_{AC}	Mean duration of the switch to emergency action	6.5 seconds

GPS system model is described with time intervals and parameter settings in Tables A-5 and A-6.

Table A-5 Time interval in GPS system

Time interval	Description
$f_E(\cdot;\ \mu_{SAT}^{down}\cdot p_{SAT}^{working}/p_{SAT}^{down})$	Time interval until the GPS system shuts down.
$f_E(\cdot;\ \mu_{SAT}^{down})$	Time interval until the GPS system recovers after the GPS system shuts down.

$f_E(\cdot;\ \mu_{SAT}^{corrupted} \cdot p_{SAT}^{working}/p_{SAT}^{corru}$	Time interval until the GPS system is corrupted.
$f_E(\cdot;\ \mu_{SAT}^{corrupted})$	Time interval until the GPS system recovers after the GPS system is corrupted.

Table A-6 Parameters in GPS system

Parameters	Explanation	Value
μ_{SAT}^{down}	Mean duration of GPS system shutting down	1/2 hour
$\mu_{SAT}^{corrupted}$	Mean duration of the GPS system recovering from it's corruption	1/2 hourr
p_{SAT}^{down}	Probability of the GPS system shutting down	10^{-5}
$p_{SAT}^{corrupted}$	Probability of the GPS becoming corrupted.	10^{-20}

GPS receiver model describes time intervals and parameter settings in Table A-7 and A-8.

Table A-7 Time interval in GPS receiver

Time interval	Description
$f_E(\cdot;\ \mu_{GPS}^{down}(1-p_{GPS}^{down})/\ p_{GPS}^{down})$	Time interval until the GPS receiver stops working.
$f_E(\cdot;\ \mu_{GPS}^{down})$	Time interval until the GPS receiver starts working again.

Table A-8 Parameters in GPS receiver

Parameter	Description	Value
μ_{GPS}^{down}	Mean duration until the GPS receiver starts working again	500 seconds
$p_{ADS,TRM}^{down}$	Probability of the GPS receiver shutting down	1/20000

Air sensor model describes time intervals and parameter settings in Tables A-9 and A-10.

Table A-9 Time interval in air sensor

Time interval	Description
$f_E(\cdot;\ \mu_{ALT}^{down}(1-p_{ALT}^{down})/\ p_{ALT}^{down})$	Time interval until the air sensor stops working.
$f_E(\cdot;\ \mu_{ALT}^{down})$	Time interval until the air sensor starts working again.

Table A-10 Parameters in air sensor

Parameter	Description	Value
μ_{ALT}^{down}	Mean duration until the air sensor starts working again	1/2 hour
p_{ALT}^{down}	Probability of the air sensor shutting down	1/20000

Horizontal estimate model describes horizontal position and speed estimation errors in three situations, when GPS is working well, corrupted, and switched to IRS estimate. GPS estimation errors are given by a normal distribution using parameters in Table A-11. IRS estimations are described following Ref. [21].

Table A-11 Parameters in horizontal estimate

Parameter	Description	Value
σ_x^{GPS}	Standard deviation of horizontal position error when the GPS is working well.	20 m
σ_v^{GPS}	Standard deviation of horizontal velocity error when the GPS is working well.	2 m/s
$\sigma_x^{GPS,DC}$	Standard deviation of horizontal position error the GPS is corrupted.	20 m
$\sigma_v^{GPS,DC}$	Standard deviation of horizontal velocity error when the GPS is corrupted.	10 m/s

Vertical estimate model describes vertical position and speed estimation errors in two situations, when vertical estimates are correct or degraded. The values of vertical estimation errors are described by stochastic differential equations and parameters are shown in Tables A-12 and A-13.

Table A-12 Stochastic differential equations in vertical estimate

Stochastic differential equation	Descriptions
$d\epsilon_t^{est,ver} = \begin{pmatrix} 0 & 1 \\ a_x & a_v \end{pmatrix} \epsilon_t^{est,ver} dt + \begin{pmatrix} 0 \\ b \end{pmatrix} d\omega_t$ $dx_t = \begin{pmatrix} 0 & 1 \\ c_x & c_v \end{pmatrix} x_t dt + \begin{pmatrix} 0 \\ c_2 \end{pmatrix} d\omega_t$	Vertical estimate errors when the altimeter is working well.
$d\epsilon_t^{est,ver} = \begin{pmatrix} 0 & 1 \\ a_x^{degr} & a_v^{degr} \end{pmatrix} \epsilon_t^{est,ver} dt + \begin{pmatrix} 0 \\ b \end{pmatrix} d\omega_t$ $dx_t = \begin{pmatrix} 0 & 1 \\ c_x^{degr} & c_v^{degr} \end{pmatrix} x_t dt + \begin{pmatrix} 0 \\ c_2 \end{pmatrix} d\omega_t$	Vertical estimate errors when the altimeter is degraded.

Here

$$\epsilon_t^{est,ver} \equiv \left[\epsilon_{t,\perp}^{est,ver},\ \ v_{t,\perp}^{est,ver}\right]^T$$
$$x_t \equiv [a_t^{est},\ \ \eta_t]^T$$

$$a_x = -(\sigma_v^{ver})^2/(\sigma_x^{ver})^2,\ a_v = -\frac{1}{2}b^2/(\sigma_v^{ver})^2$$
$$a_x^{degr} = -\left(\sigma_v^{ver,degr}\right)^2/\left(\sigma_x^{ver,degr}\right)^2,\ a_v^{degr} = -\frac{1}{2}b^2/\left(\sigma_v^{ver,degr}\right)^2$$
$$c_x = -(\sigma_2/\sigma_1)^2,\ c_v = -\frac{1}{2}(c_2/\sigma_2)^2$$

$c_x^{degr} = -\left(\sigma_2^{degr}/\sigma_1^{degr}\right)^2$, $c_v^{degr} = -\frac{1}{2}\left(c_2/\sigma_2^{degr}\right)^2$

Table A-13 Parameters in vertical estimate

Parameters	Explanation	Value
σ_x^{ver}	Standard deviation of vertical position error when the altimeter is working well	10 m
σ_v^{ver}	Standard deviation of vertical velocity error when the altimeter is working well	1 m/s
$\sigma_x^{ver,degr}$	Standard deviation of vertical position error when the altimeter is degraded or corrupted	60 m
$\sigma_v^{ver,degr}$	Standard deviation of vertical velocity error when the altimeter is degraded or corrupted	2 m/s
σ_1	Standard deviation of TAS evaluation error in correct mode	1 m/s
σ_1^{degr}	Standard deviation of TAS evaluation error in degraded mode	1 m/s
σ_2	Standard deviation of TAS derivative evaluation error in correct mode	0.1 m/s
σ_2^{degr}	Standard deviation of TAS derivative evaluation error in degraded mode	0.1 m/s
b	Noise level	1
c_2	Noise level of airspeed	0.05

The exponential distribution f_E is defined as:

$$f_E(x;\,\mu) = \frac{1}{\mu} exp\left(\frac{-x}{\mu}\right),\ \ x \geq 0 \qquad \text{(A-1)}$$

The Rayleigh distribution f_R is defined as:

$$f_R(x;\,\mu) = 2\rho x\ exp(-\rho x^2),$$

$$\rho = \frac{\pi}{4\mu^2}, x \geq 0 \qquad \text{(A-2)}$$

Contact Author Email Address

Eri Itoh: eri@enri.go.jp

Copyright Statement